

Proteomic profiling of sporadic late-onset nemaline myopathy

Elie Naddaf¹ , Surendra Dasari², Duygu Selcen¹, M. Cristine Charlesworth³, Kenneth L. Johnson³, Michelle L. Mauermann¹ & Taxiarchis Kourelis⁴

¹Division of Neuromuscular Medicine, Department of Neurology, Mayo Clinic, Rochester, Minnesota, USA

²Department of Qualitative Health Sciences, Mayo Clinic, Rochester, Minnesota, USA

³Medical Genome Facility Proteomics Core, Mayo Clinic, Rochester, Minnesota, USA

⁴Division of Hematology, Department of Internal Medicine, Mayo Clinic, Rochester, Minnesota, USA

Correspondence

Elie Naddaf, Department of Neurology, Mayo Clinic, 200 First Street Southwest, Rochester, MN 55905. Tel: 507-282-2120; Fax: 507-538-6012; E-mail: naddaf.elie@mayo.edu

Received: 7 January 2022; Accepted: 4 February 2022

Annals of Clinical and Translational Neurology 2022; 9(3): 391–402

doi: 10.1002/acn3.51527

Funding Information

The study was funded by the Department of Neurology Discretionary Funds at Mayo Clinic, Rochester.

Abstract

Objective: To define the proteomic profile of sporadic late-onset nemaline myopathy (SLONM) and explore its pathogenesis. **Methods:** We performed mass spectrometry on laser-dissected frozen muscle samples from five patients with SLONM, three of whom with an associated monoclonal protein (MP), and four controls, to determine the proteomic profile of SLONM. Furthermore, we assessed the role of the MP by evaluating the expression of the immunoglobulin light chain variable regions (IGVL). **Results:** There were 294 differentially expressed proteins: 272 upregulated and 22 downregulated. Among the top 100 upregulated proteins, the most common categories were: nuclear or nucleic acid metabolism (24%), extracellular matrix and basal lamina (17%), immune response (13%), and actin dynamics (8%). Downregulated proteins consisted mostly of contractile proteins. Among upregulated proteins, there were 65 with a role related to the immune system, including eight proteins involved in major histocompatibility complex 1 (MHC1) and antigen processing, 15 in MHCII complex and phagocytosis, and 23 in B and/or T-cell function. Among nine upregulated immunoglobulin proteins, there were two IGVL genes. However, these were also detected in SLONM cases without an MP, with no evidence of clonally dominant immunoglobulin deposition. In muscle sections from SLONM patients, nemaline rods tended to accumulate in atrophic fibers with marked rarefaction of the myofibrils. Increased MHC1 reactivity was present in fibers containing nemaline rods as well as adjacent nonatrophic fibers. **Conclusion:** Our findings suggest that aberrant immune activation is present in SLONM, but do not support a direct causal relationship between the MP and SLONM.

Introduction

Sporadic late-onset nemaline myopathy (SLONM) is a rare acquired myopathy that affects adults, usually after the age of 40.^{1,2} Muscle weakness can be rapidly progressive, and lead to respiratory failure and death if left untreated.^{3–5} About 61% of patients have an associated monoclonal protein (MP).¹ A causal relationship between the plasma cell disorder and SLONM has not been well established, especially since MPs are also identified in 3–5% of the general population of the same age.⁶ However,

the higher than expected frequency of an MP in SLONM raises suspicion for association between the two entities.^{1,2} Except in rare cases, the MP in SLONM is classified as monoclonal gammopathy of uncertain significance (MGUS), and patients usually die from neuromuscular respiratory failure rather than from progression to hematologic malignancies.⁵ Fortunately, when accurately diagnosed, the majority of patients respond to treatment with intravenous immunoglobulin.^{1,7} In patients with an associated MP, autologous stem cell transplant (ASCT) or plasma cell-directed therapy may also be considered.^{1,2,8,9}

On the other hand, treatment response to corticosteroids or oral immunosuppressant's remains poor.^{1,5}

Histologically, SLONM is characterized by accumulation of nemaline rods in muscle fibers with minimal or no inflammation.^{3,4,10} Aside from its response to IVIG and ASCT, it remains uncertain whether the disease is immune mediated, and little is known regarding the underlying disease mechanisms. In this study, we performed laser dissection liquid chromatography and electrospray tandem mass spectrometry (LMD-MS) to define the proteomic composition of SLONM and shed light into its pathogenesis.

Methods

Selection of cases and controls

The study was approved by Mayo Clinic Institutional Review Board. The study was considered minimal risk; therefore, the requirement for informed consent was waived. However, records of any patient who had not provided authorization for their medical records to be used for research, as per Minnesota statute 144.335, were not reviewed. Patients with SLONM were identified from our recently published cohort.¹ We selected five patients with SLONM who were not on immunosuppression for their myopathy at time of the biopsy, and who had remaining frozen muscle tissue. We identified four controls from our muscle laboratory database. To be included as a control, the patient had to have no clinical evidence of a myopathy and normal creatine kinase level.

Processing of muscle samples

Fibers with nemaline rods from SLONM patients and normal muscle fibers from controls were collected in separate tubes by laser pressure catapulting (LPC) using a Zeiss Palm MicroBeam scope controlled by RoboPalm software. In order to do that, 10 μm sections of frozen muscle on polyethylene naphthalate membrane slides (ThermoFisher Scientific, Waltham, MA) were stained with trichrome to visualize fibers with rod aggregation. Fibers with rods were outlined, laser microdissected, and catapulted into the cap of 0.5 mL tubes containing 0.05% Protease Max/0.005% Zwittergent 3–16/100 mmol/L Tris, pH 8.5. Nuclei were avoided where possible. Similar process was applied to sections from controls containing structurally normal fibers. An area of 0.3 mm^2 was collected for each sample. Samples were trypsin-digested in the same collection tube after protein reduction and alkylation. After acidification, each peptide digest was transferred to a mass spectrometry (MS) sample vial, dried

down, and brought up in the same volume of 0.1% trifluoroacetic acid for injection on the MS.

Label-free liquid chromatography MS

Digested samples were loaded onto an nLC–MS/MS system consisting of a Q-Exactive Orbitrap high resolution mass spectrometer and a Dionex Ultimate 3000 RSLC nano liquid chromatograph (nLC) (ThermoFisher Scientific, Waltham, MA). Peptides were pre-concentrated onto a 0.33- μL EXP2 trap (2.7 μm Halo Peptide ES-C18, Optimize Technologies, Oregon City, OR) in the Dionex column oven and washed using a 10- $\mu\text{L}/\text{min}$ flow of aqueous 0.05% TFA and 0.2% formic acid before switching the trap in-line with the nLC column. Peptides were separated on a 35 cm long \times 75 μm id PicoFrit column, self-packed with ThermoFisher Acclaim RSLC 2.2 μm C18 stationary phase, using a 120 min reversed phase LC method with a gradient from 2% to 40% B in 100 min at 250 nL/min flow rate, followed by increasing to 85% B for 6 min before re-equilibrating the column and trap at 2% B. Mobile phase A was 2% acetonitrile in water with 0.2% formic acid; mobile phase B was 80% acetonitrile, 10% isopropanol, and 10% water with 0.2% overall concentration of formic acid. The trap and column were heated to 40°C.

MS and MS/MS spectra were acquired in a data-dependent acquisition mode with MS precursors acquired from m/z 340 to 1800 (60,000 resolving power (RP) FWHM at m/z 200, AGC = 3e6, max fill time = 150 msec). MS/MS spectra were collected for the top 20 precursors with charge 2–5, at a normalized collision energy = 26 (15,000 RP, AGC = 1e5, max fill time = 80 msec, isolation window = 3, window offset = 0.5, fixed first m/z of 140, precursor dynamic exclusion = 30 sec).

Bioinformatics and statistical analysis

A previously published bioinformatics pipeline was utilized to process the raw LC–MS/MS data and perform peptide intensity-based label-free quantification of proteins present in the samples.¹¹ Raw data files were loaded into MaxQuant software (version 1.6.0.16) configured to search the MS/MS spectra against a database containing Uniprot human protein sequences (downloaded on 20 November 2020) and common contaminants (like sheep keratin, cotton proteins, etc.).¹² Reversed protein sequences were appended to the database to estimate peptide and protein false discovery rates (FDRs). MaxQuant was instructed to use trypsin as digestion enzyme and the following posttranslational modifications when matching the MS/MS against the sequence database:

carbamidomethyl cysteine (+57.021 Da), oxidation of methionine (+15.995), and deamidation of asparagine (+0.985). The software identified the peptides and proteins present in the samples at an FDR $\leq 1\%$, grouped protein identifications into groups and reported protein group intensities.

A previously published, in-house developed R script was utilized to process the reported protein group intensities and find differentially expressed proteins between any two experimental groups (Data S1).¹¹ For this, protein group intensities of each sample were log₂ transformed and normalized using trimmed mean of M-values method. For each protein group, the normalized intensities observed in any two experimental groups of samples were modeled using a Gaussian-linked generalized linear model. An ANOVA test was utilized to detect the differentially expressed protein groups between pairs of experimental groups. Differential expression *p*-values were FDR corrected using Benjamini–Hochberg–Yekutieli procedure. Protein groups with an FDR < 0.05 and an absolute log₂ fold change of at least 0.5 were considered as significantly differentially expressed and saved for further analysis.

Investigation of immune system-related proteins

We investigated the role of each of the top 100 upregulated proteins and the 22 downregulated proteins via literature search. To further investigate the potential immune basis of SLONM, we also searched the immune role of all the differentially expressed proteins of interest. These proteins were identified from immune-related pathways detected by Broad's Gene Set Enrichment Software¹³ and Ingenuity Pathway analysis software.

Assessment of immunoglobulin clonality

In order to determine the role of the MP in SLONM and the clonality of the detected immunoglobulins in muscle, we searched the raw data files against a light chain variable region (IGVL) sequence database as previously described.¹⁴ IGVLs are unique for each plasma cell clone and can therefore be used as a surrogate for clonality of the deposited immunoglobulins. In brief, a database of immunoglobulin light chain variable genes was assembled and the MS/MS spectra in each sample were matched against the database using MyriMatch database search engine. Reversed sequence entries were appended to the database to estimate FDRs. MyriMatch was configured to use the same peptide/fragment mass tolerances, digestion enzyme, and posttranslational modifications as the MaxQuant-based procedure described above. IDPicker software was utilized to filter the peptide and protein

identifications at 1% FDR. Identified peptides that matched to light/heavy chain constant/variable regions were grouped by their gene family and their MS/MS counts were added together. Spectral counts of each Ig gene were normalized, as previously described.¹⁵ A Wilcoxon rank test was used to evaluate for differential expression of Ig genes between the two experimental groups, and genes with a *p*-value < 0.05 were considered as statistically significant. We also computed the log₂ ratio of average counts observed for each Ig gene in samples from SLONM patients versus control subjects.

Immunohistochemical and immunofluorescence studies

Major histocompatibility complex class I (MHC1) was immunolocalized using monoclonal antibodies on frozen sections from the five included SLONM patients and controls. We also included five patients from our database with congenital nemaline myopathy. Consecutive trichrome-stained sections were performed to identify the fibers with nemaline rods. Capillary endothelia were localized with *Ulex europaeus* agglutinin I (UEA), and the complement C5b9 membrane attack complex (MAC) with monoclonal antibodies in frozen sections from patients and controls and visualized under immunofluorescence microscopy.

Data availability

Data not provided in the article and additional information on methods and materials may be shared upon request.

RESULTS

Baseline characteristics of patients and controls

The demographics and disease characteristics of patients with SLONM are shown in Table 1. Controls had a median age of 52 (range 40–60) and included two males and two females. The muscle biopsies were obtained to rule out a myopathy for the following symptoms: myalgia (two patients), dyspnea on exertion, and fatigue.

Proteomics

Of the 1458 total detected proteins, 294 proteins were differentially expressed in SLONM, of which 272 upregulated and 22 downregulated. Among the top 100 upregulated proteins, the most common categories were as follows: nuclear or nucleic acid metabolism (24%),

Table 1. Baseline characteristics of patients with sporadic late-onset nemaline myopathy.

	All patients	P1	P2	P3	P4	P5
Age at biopsy	59 (48–68)	59	46	58	63	68
Sex	4M/1F	M	M	F	M	M
Disease duration (symptom onset to biopsy date)	23 (4–138)	39	6	4	138	23
Associated monoclonal protein	3/5 (60%)	N	Y	N	Y	Y

F, female; M, male.

extracellular matrix and basal lamina (17%), and immune response (13%) (Table 2). Downregulated proteins consisted mostly of contractile proteins. A complete list of differentially expressed proteins is shown in Table S1.

Proteins related to the immune system

Among 272 upregulated proteins, 65 unique proteins play a role related to the immune system, some with overlapping roles (Table 3). Eight proteins are involved in MHC1 and antigen processing, 15 in MHCII antigen presentation and phagocytosis, and 23 in B and/or T-cell function. Furthermore, C9 was upregulated, in addition to 22 proteins with various other immune roles.

Assessment of immunoglobulin clonality

There were nine upregulated immunoglobulin proteins in muscles of SLONM patients: five heavy chain constant region proteins (IGHG1-02, IGHG1-03, IGHG2-02, IGHG3-03, and IGHG4-02), two heavy chain variable region proteins (IGHV3-30 and IGHV3-74), and two light chain variable region proteins (IGKV3-11 and IGKV3-20). Detailed results are shown in Table S2. As mentioned in the methods section, IGVLs are unique to each plasma cell clone and they serve as surrogates of immunoglobulin clonality. Log₂ fold ratio for SLONM versus controls was 1.64 IGKV3-20 and 1.07 for IGKV3-11. Upregulation of IGKV3-20 was seen in all samples from SLONM patients, with or without an MP.

Immunohistochemical studies

Given the upregulation of proteins of the MHC1 complex in our cases, we aimed to confirm this finding by immunohistochemistry and to evaluate if it is helpful in differentiating SLONM from congenital nemaline myopathy. Therefore, we evaluated our cases and five patients

with congenital nemaline myopathy for MHC1 expression. The latter included: two 31- and 19-year-old females with ACTA1 myopathy and a 1 year-old female, a 3-year-old male, and a 2-month-old male with unknown genes. In SLONM, nemaline rods tend to accumulate in atrophic fibers with marked rarefaction of the myofibrils. Whereas in congenital nemaline myopathies, nemaline rods occur in nonatrophic fibers and are located subsarcolemmally or scattered throughout the sarcoplasm (Fig. 1). In muscle specimens from patients with SLONM, increased MHC1 reactivity was present in fibers containing nemaline rods, as well as adjacent nonatrophic fibers without structural abnormalities or rod accumulation (Fig. 1). This pattern was seen in four out of five SLONM patients and the fifth patient had scattered muscle fibers with increased MHC1 reactivity. In contrast, fibers containing nemaline rods from patients with congenital nemaline myopathy did not display increased MHC1 reactivity (Fig. 1). There was no evidence of a microangiopathy on UEA staining, and only rare fibers had sarcolemmal complement deposit on MAC staining (data not shown). Of note, none of the SLONM patients had inflammatory collections on muscle biopsy.

Discussion

In this study, we provided a descriptive overview of the proteomic profile of SLONM and we highlighted the immune-mediated pathways. Our results suggest that despite the lack of inflammatory collections on muscle biopsy, several immune-related proteins in muscle samples obtained from patients with SLONM are upregulated, including those related to MHC-1 antigen processing and antibody-mediated damage. Furthermore, there was no evidence of direct deposition of MP in muscle tissue.

MHC1 upregulation allows a nucleated cell to present antigens recognized by T-lymphocytes.¹⁶ MHC1 and several related proteins were upregulated in SLONM, including proteins involved in MHC1 processing in the endoplasmic reticulum such as β 2-microglobulin, calnexin, calreticulin, and PDIA3; and antigen processing by proteasomal enzymes such as LMO7, PSMD1, and PSMD3. The MHC1/antigen complex is then presented at the cell membrane (sarcolemmal MHC1 reactivity on immunohistochemistry). The MHC1/antigen complex interacts with the corresponding CD8 T-cell via two main receptors: the CD8 receptor or and the T-cell receptor (TCR). Among the CD8 T-cell-related upregulated proteins, several of which are involved in TCR activation and signaling such as HNRNPU, DBNL, PSMD3, and PSMD1.^{17,18} We also identified several proteins involved in B-cell function and signaling, most prominent among

Table 2. Top 100 upregulated and all downregulated proteins.

Gene	Protein name	Log2 fold change	Gaussian FDR
Nuclear or nucleic acid metabolism			
<i>HNRNPU</i>	Heterogeneous nuclear ribonucleoprotein U	37.6845	0
<i>HNRNPC</i>	Heterogeneous nuclear ribonucleoprotein C1/2	37.4689	0
<i>XRCC6</i>	X-ray repair cross-complementing protein 6	37.3472	0
<i>LMO7</i>	LIM domain only protein 7	37.2114	2.10E-117
<i>HNRNPA3</i>	Heterogeneous nuclear ribonucleoprotein A3	36.7089	0
<i>H1FO</i>	Histone H1.0	36.6937	1.92E-61
<i>DDX17</i>	Probable ATP-dependent RNA helicase DDX17	36.4066	0
<i>MATR3</i>	Matrin-3	35.9364	4.32E-90
<i>XRCC5</i>	X-ray repair cross-complementing protein 5	35.8049	0
<i>CRIP2</i>	Cysteine-rich protein 2	35.4522	0
<i>SFPQ</i>	Short of Splicing factor, proline-and glutamine-rich	34.8728	1.31E-228
<i>IMPDH2</i>	Inosine-5'-monophosphate dehydrogenase 2	34.8171	0
<i>HNRNPR</i>	Heterogeneous nuclear ribonucleoprotein R	34.6812	1.06E-207
<i>RBMX</i>	RNA-binding motif protein, X chromosome	34.5301	4.93E-250
<i>EIF3L</i>	Eukaryotic translation initiation factor 3 subunit L	34.2818	4.61E-157
<i>EIF3C</i>	Eukaryotic translation initiation factor 3 subunit C	34.0884	5.02E-220
<i>TNPO1</i>	Transportin-1	34.0577	0
<i>TARDBP</i>	TAR DNA-binding protein 43	33.9986	0
<i>HDGF</i>	Hepatoma-derived growth factor	32.9447	3.15E-198
<i>NCL</i>	Nucleolin	32.5568	1.70E-05
<i>HNRNPH1</i>	Heterogeneous nuclear ribonucleoprotein H	30.2065	0.0009048
<i>HNRNPM</i>	Heterogeneous nuclear ribonucleoprotein M	29.1451	0.003114204
<i>HNRNPAB</i>	Heterogeneous nuclear ribonucleoprotein A/B	27.9319	0.003636039
<i>SUN2</i>	SUN domain-containing protein 2	27.8461	0.003623759
<i>TMEM43</i>	Transmembrane protein 43	27.4371	0.000481811
<i>SMYD1</i>	Histone-lysine N-methyltransferase SMYD1	-3.5626	0.00296268
Contractile proteins			
<i>MYOM3</i>	Myomesin-3	37.1096	4.70E-303
<i>MYO18B</i>	Unconventional myosin-XVIIIb	36.5623	0
<i>MYL6</i>	Myosin light polypeptide 6	29.8760	0.000987854
<i>TNNC1</i>	Troponin C, slow skeletal and cardiac muscles	-2.5635	0.000239163
<i>TPM3</i>	Tropomyosin alpha-3 chain	-2.7234	0.000811562
<i>MYBPC1</i>	Myosin-binding protein C, slow-type	-3.4846	7.70E-05
<i>TPM2</i>	Tropomyosin beta chain	-3.6542	0.006675157
<i>TTN</i>	Titin	-3.7723	1.25E-05
<i>MYOM1</i>	Myomesin-1	-3.9935	0.004184786
<i>MYL1</i>	Myosin light chain 1/3, skeletal muscle	-4.0273	0.007628146
<i>MYL2</i>	Myosin regulatory light chain 2	-4.0926	0.001551271
<i>MYL5</i>	Myosin light chain 5	-5.4719	0.003475986
<i>MYL3</i>	Myosin light chain 3	-5.5703	0.009064135
<i>MYH1</i>	Myosin-1	-5.7091	0.001422474
<i>MYBPC2</i>	Myosin-binding protein C, fast-type	-5.8789	0.003197956
<i>MYH13</i>	Myosin-13	-5.9548	1.20E-07
<i>MYOM2</i>	Myomesin-2	-6.7592	8.61E-13
<i>MYLPF</i>	Myosin regulatory light chain 2, skeletal muscle isoform	-7.1407	0.001092562
<i>MYBPC1</i>	Myosin-binding protein C, slow-type	-29.8774	0.000435494
Extracellular matrix/basal lamina			
<i>POSTN</i>	Periostin	38.1531	5.29E-77
<i>NID2</i>	Nidogen	37.8429	0
<i>PRELP</i>	Prolargin	36.2660	4.02E-66
<i>MFAP5</i>	Microfibrillar-associated protein 5	35.8636	2.68E-109
<i>COL15A1</i>	Collagen alpha-1(XV) chain	35.1866	8.55E-227
<i>CILP</i>	Cartilage intermediate layer protein 1	35.0617	5.31E-247
<i>TGFBI</i>	Transforming growth factor-beta-induced protein Ig-H3	34.8320	3.38E-136

(Continued)

Table 2 Continued.

Gene	Protein name	Log2 fold change	Gaussian FDR
<i>FBLN2</i>	Fibulin-2	34.2103	5.77E-121
<i>EPDR1</i>	Mammalian ependymin-related protein 1	34.0783	0
<i>BGN</i>	Biglycan	34.0641	0
<i>FBLN5</i>	Fibulin-5	29.4811	0.000667082
<i>DPT</i>	Dermatopontin	28.9198	0.003623759
<i>COL2A1</i>	Collagen alpha-1(II) chain	28.4937	0.003636039
<i>ELN</i>	Elastin	27.8247	0.003636039
<i>MFAP4</i>	Microfibril-associated glycoprotein 4	27.6941	0.003852888
<i>TNS1</i>	Tensin-1	27.4890	0.003623759
<i>OGN</i>	Mimecan	27.3773	0.002134546
Immune response			
<i>B2M</i>	Beta-2-microglobulin	37.1546	5.21E-132
<i>ILF2</i>	Interleukin enhancer-binding factor 2	33.9899	0
<i>C9</i>	Complement component C9	33.9726	0
<i>ORM1</i>	Alpha-1-acidglycoprotein1	33.9338	3.31E-124
<i>HLA-A</i>	HLA class I histocompatibility antigen, A alpha chain	33.6618	4.12E-171
<i>ILF3</i>	Interleukin enhancer-binding factor 3	32.7224	0
<i>IGHM</i>	Immunoglobulin heavy constant Mu	29.2927	0.003636039
<i>IGKV3D-20</i>	Immunoglobulin kappa variable 3D-20	28.9261	0.003636039
<i>AMBP</i>	Alpha-1-microglobulin/Bikunin precursor	28.7914	0.003623759
<i>IGKV2-29</i>	Immunoglobulin kappa variable 2-29	28.7343	0.004076039
<i>AHSG</i>	Alpha-2-HS-glycoprotein	28.4887	0.004105626
<i>IGKV1-33</i>	Immunoglobulin kappa variable 1-33	28.3757	0.003642231
<i>GBP1</i>	Guanylate-binding protein 1	27.9825	0.004076039
Actin dynamics			
<i>CCT4</i>	T-complex protein 1 subunit delta	36.2017	1.23E-220
<i>CALD1</i>	Caldesmon	31.0103	0
<i>MYL12A</i>	Myosin regulatory light chain 12A	30.7955	0.000547829
<i>ABLIM1</i>	Actin-binding LIM protein 1	30.5517	0.001530352
<i>EPS8L2</i>	Epidermal growth factor receptor kinase substrate 8-like protein 2	29.0159	0.004255693
<i>ACTR3</i>	Actin-related protein 3	28.0870	0.000859807
<i>SEPTIN7</i>	Septin-7	27.7239	0.003636039
<i>DIAPH1</i>	Protein diaphanous homolog 1	27.5552	0.004105626
Protein homeostasis			
<i>PSAP</i>	Prosaposin	39.3859	0
<i>RPN2</i>	Dolichyl-diphosphooligosaccharide--proteinglycosyltransferase subunit 2	34.1529	0
<i>HSP90B1</i>	Endoplasmic	28.9454	0.00101187
<i>LMAN2</i>	Vesicular integral-membrane protein VIP36	28.0242	0.00374991
<i>VPS35</i>	Vacuolar protein sorting-associated protein 35	27.8197	0.003814025
<i>CES2</i>	Cocaine esterase	27.7888	0.003075447
<i>CMBL</i>	Carboxymethylenebutenolidase homolog	-4.1632	6.51E-06
Cytoskeleton			
<i>SYNC</i>	Syncoilin	36.4357	1.55E-290
<i>MAPRE1</i>	Microtubule-associated protein RP/EB family member 1	33.8011	2.49E-196
<i>LAMA5</i>	Laminin subunit alpha-5	33.7594	0
<i>NES</i>	Nestin	33.6240	9.13E-05
<i>CNTRL</i>	Centriolin	-28.5006	0.000638065
Ribosome			
<i>RPS4X</i>	40S ribosomal protein S4	34.4797	1.10E-87
<i>RPL15</i>	60S ribosomal protein L15	31.6865	1.61E-87
<i>RPS17</i>	40S ribosomal protein S17	28.7062	0.000771255
<i>RPL14</i>	60S ribosomal protein L14	27.8408	0.003636039
Metabolism/mitochondria			
<i>ADH1B</i>	All-trans-retinol dehydrogenase [NAD(+)]ADH1B	37.0445	0
<i>STOML2</i>	Stomatin-like protein 2, mitochondrial	34.5410	0

(Continued)

Table 2 Continued.

Gene	Protein name	Log2 fold change	Gaussian FDR
<i>PGD</i>	6-phosphogluconate dehydrogenase, decarboxylating	29.3747	0.004839224
<i>GLUD1</i>	Glutamate dehydrogenase 1, mitochondrial	29.1598	7.40E-05
Cytoplasmic vesicles			
<i>ARF5</i>	ADP-ribosylation factor 5	37.1513	6.17E-186
<i>EHD2</i>	EH domain-containing protein2	35.8474	0
<i>RAB11A</i>	Ras-related protein Rab-11A	34.3366	2.80E-255
<i>DYNC1I2</i>	Cytoplasmic dynein 1 intermediate chain 2	28.1554	0.000402775
Calcium homeostasis			
<i>S100A4</i>	Protein S100-A4	37.1418	6.41E-96
<i>S100A1</i>	Protein S100-A1	-3.8520	0.002102357
Sarcolemmal			
<i>SGCG</i>	Gamma-sarcoglycan	29.1324	0.000330293
<i>CLIC1</i>	Chloride intracellular channel protein 1	28.4947	0.003924595
Others			
<i>ATP1A1</i>	Sodium/potassium-transporting ATPase subunit alpha-1	35.4325	0
<i>RRAD</i>	GTP-binding protein RAD	35.2894	2.22E-250
<i>GNA13</i>	Guanine nucleotide-binding protein subunit alpha-13	33.1138	1.72E-48
<i>FTL</i>	Ferritin light chain	29.7657	0.000893115
<i>NIBAN2</i>	Protein Niban 2	29.0158	0.004255693
<i>A2M</i>	Alpha-2-macroglobulin	28.6148	0.002652335
<i>TTR</i>	Transthyretin	28.2200	0.003860949
<i>A1BG</i>	Alpha-1B-glycoprotein	27.6996	0.003636039
<i>PLCD4</i>	1-phosphatidylinositol 4,5-bisphosphate phosphodiesterase delta-4	-25.7326	0.001141208
<i>AAMDC</i>	Mth938 domain-containing protein	-28.3072	0.000637142

Proteins are shown by categories in a descending order based on the log2 fold change. Downregulated proteins have negative log2fold change values. FDR, false discovery rate.

which were several light and heavy chain components as discussed below.

The role of the MP detected in 60% of patients with SLONM is not well understood. The upregulation of nine immunoglobulin proteins is suggestive of underlying immune activation and antibody-mediated tissue damage. Here, we posit that the circulating MP, detected in patients' sera, may be a simple indicator of underlying autoimmunity rather than direct involvement of the monoclonal process in muscle damage. Indeed, inflammatory disorders are a risk factor for developing an MGUS.¹⁹ In these cases, the MP is not known to play a causal role in the development of inflammation. This is supported in this study by the absence of a clonally dominant MP at the proteomic level. This contrasts with diseases with direct deposition of clonal immunoglobulins such as AL amyloidosis, where much higher amounts of clonally deposited IGVs are typically detected.^{20,21} We also reported increased expression of IGV3-20 in SLONM patients compared to controls. This finding is more likely to represent a marker of nonspecific immune activation for several reasons. First, both SLONM patients with and without MP had higher IGKV3-20 than controls. Second, IGKV3 is a variable region gene family that is only noted

in approximately 6–7% of patients with dysproteinemias, but in about 25% of polyclonal plasma cells, making it more likely to represent polyclonal deposition in the SLONM cases.²² The reason 2 SLONM-MP cases appeared to have higher levels of several immunoglobulin heavy and light chain variable regions compared to the remaining SLONM cases may suggest that the presence of an MP is a surrogate of heightened immune-mediated muscle damage, which could explain the disease's more aggressive clinical course in some. This study also underlines the heterogeneity across SLONM-MP cases with some having immunoglobulin deposition levels comparable to that of SLONM without MP. Therefore, we continue to suggest considering a trial of IVIG first in all patients with SLONM irrespective of the presence of an MP.^{1,23}

Finally, while the protein abundance levels of cytokines and interleukins were below the current proteome depth of coverage for the LPC and proteomics methods described here, we showed upregulation of proteins related to IL2 (ILF2, ILF3), IL6 (ORM1, HNRNPK, HNRNPM), interferons (HSP90B1, GBP1), TGF- β (AHSG is a TGF- β antagonist), and IL10 (HSPA5) signaling.^{24–27} These findings raise suspicion for a Th1-mediated immune response, as seen in other immune-

Table 3. Immune system-related proteins.

Gene	Protein name	Comments
MHC1 and antigen processing		
<i>B2M</i>	Beta-2-microglobulin	MHC1 complex
<i>CALR</i>	Calreticulin	Endoplasmic reticulum processing
<i>CANX</i>	Calnexin	Endoplasmic reticulum processing
<i>HLA-A</i>	HLA class I histocompatibility antigen, A alpha chain	MHC1 complex
<i>LMO7</i>	LIM domain only protein 7	Endoplasmic reticulum processing
<i>PDIA3</i>	Protein disulfide-isomerase A3	Endoplasmic reticulum processing
<i>PSMD1</i>	26S proteasome non-ATPase regulatory subunit 1	Proteasome
<i>PSMD3</i>	26S proteasome non-ATPase regulatory subunit 3	Proteasome
MHCII and phagocytosis		
<i>ASAH1</i>	Acid ceramidase	Neutrophil degranulation
<i>CALM3</i>	Calmodulin-3	Transmembrane signaling
<i>COL1A1</i>	Collagen alpha-1(I)chain	Dendritic cell maturation
<i>COL1A2</i>	Collagen alpha-2(I) chain	Dendritic cell maturation
<i>CTSD</i>	Cathepsin	Phagosome
<i>DYNC1H1</i>	Cytoplasmic dynein 1 heavy chain 1	Phagosome
<i>DYNC1I2</i>	Cytoplasmic dynein 1 intermediate chain 2	Phagosome
<i>GBP1</i>	Guanylate-binding protein 1	Phagosome
<i>HNRNPM</i>	Heterogeneous nuclear ribonucleoprotein M	Macrophage function
<i>HSPD1</i>	60 kDa heat shock protein, mitochondrial	Macrophage function
<i>MVP</i>	Major vault protein	Neutrophil degranulation
<i>PRDX5</i>	Peroxiredoxin-5, mitochondrial	Phagosome
<i>PSAP</i>	Prosaposin	Neutrophil degranulation
<i>RAB11A</i>	Ras-related protein Rab-11A	Phagosome
<i>VAPA</i>	Vesicle-associated membrane protein-associated protein A	Macrophage function
T cells		
<i>ACTR3</i>	Actin-related protein 3	CD28 Signaling in T-Helper Cells
<i>AHSG</i>	Alpha-2-HS-glycoprotein	T-cell activation, inhibits TGF- β
<i>ANXA5</i>	Annexin A5	Immune checkpoint inhibitor
<i>CALM3</i>	Calmodulin-3	Transmembrane signaling
<i>DBNL</i>	Drebrin-like protein	T-cell activation, TCR related
<i>HNRNPU</i>	Heterogeneous nuclear ribonucleoprotein U	TCR-dependent signaling and activation
<i>HSP90AB1</i>	Heat shock protein HSP90-beta	T-cell-mediated antitumor responses
<i>HSP90B1</i>	Endoplasmic	T-cell-mediated antitumor responses
<i>ILF2</i>	Interleukin enhancer-binding factor 2	Required for T-cell expression of interleukin 2
<i>ILF3</i>	Interleukin enhancer-binding factor 3	Required for T-cell expression of interleukin 2
<i>PADI2</i>	Protein-arginine deiminase type-2	Regulates Th2 and Th17 T cells
<i>PCBP1</i>	Poly(rC)-binding protein 1	Immune checkpoint for T cells
<i>PSMD1</i>	26S proteasome non-ATPase regulatory subunit 1	TCR signaling
<i>PSMD3</i>	26S proteasome non-ATPase regulatory subunit 3	TCR signaling
<i>RAC1</i>	Ras-related C3 botulinum toxin substrate 1	Transmembrane signaling in B and T cells
B cells		
<i>CALM3</i>	Calmodulin-3	Transmembrane signaling
<i>CDC42</i>	Cell division control protein 42 homolog	Essential for the Activation and Function of Mature B Cells
<i>HNRNPC</i>	Heterogeneous nuclear ribonucleoprotein C1/2	Follicular B cell maintenance
<i>IGHG2</i>	Immunoglobulin heavy constant gamma 2	Plasma cells
<i>IGHM</i>	Immunoglobulin heavy constant Mu	Plasma cells
<i>IGKC</i>	Immunoglobulin kappa constant	Plasma cells

(Continued)

Table 3 Continued.

Gene	Protein name	Comments
<i>IGKV1-33</i>	Immunoglobulin kappa variable 1–33	Plasma cells
<i>IGKV2-29</i>	Immunoglobulin kappa variable 2–29	Plasma cells
<i>IGKV3D-20</i>	Immunoglobulin kappa variable 3D-20	Plasma cells
<i>RAC1</i>	Ras-related C3 botulinum toxin substrate 1	Transmembrane signaling in B and T cells
Miscellaneous		
<i>C9</i>	Complement component C9	Membrane attack complex
<i>FTL</i>	Ferritin light chain	Acute phase reactant
<i>A1BG</i>	Alpha-1B-glycoprotein	Sequence similarity to the variable regions of some immunoglobulin supergene family member proteins.
<i>A2M</i>	Alpha-2-macroglobulin	Acute phase reactant
<i>AMBP</i>	Alpha-1-microglobulin/Bikunin precursor	Acute phase reactant
<i>APCS</i>	Serum amyloid P-component	Acute phase reactant
<i>ARHGAP1</i>	Rho GTPase-activating protein 1	Rho signaling pathway
<i>BGN</i>	Biglycan	Regulates inflammation and innate immunity
<i>DCD</i>	Dermcidin	Antimicrobial
<i>GNA13</i>	Guanine nucleotide-binding protein subunit alpha-13	Rho signaling pathway
<i>GSN</i>	Gelsolin	Acute phase reactant
<i>HIST1H4A</i>	Histone H4	Immune system activation
<i>HIST2H2AA3PE</i>	Histone H2A type2-A	Immune system activation
<i>HIST2H2BE</i>	Histone H2B type2-E	Immune system activation
<i>HNRNPK</i>	Heterogeneous nuclear ribonucleoprotein K	Acute phase reactant. Inhibits NF-IL6
<i>HSPA5</i>	Endoplasmic reticulum chaperone BIP	Promotes the production of anti-inflammatory cytokines by interacting with phagocytic cells
<i>ORM1</i>	Alpha-1-acidglycoprotein1	Acute phase reactant, inhibits NF-IL6
<i>TF</i>	Serotransferrin	Acute phase reactant
<i>TLN1</i>	Talin-1	Attachment of lymphocytes to the extracellular matrix
<i>TTR</i>	Transthyretin	Acute phase reactant
<i>XRCC5</i>	X-ray repair cross-complementing protein 5	Innate immune response activation, cGAS pathway
<i>XRCC6</i>	X-ray repair cross-complementing protein 6	Innate immune response activation, cGAS pathway

MHC1, major histocompatibility complex 1; TCR, T-cell receptor.

mediated myopathies.^{28–30} It is noteworthy that some proteins although not classically classified as immune proteins play a role in the immune system. Heat shock proteins are implicated in both pro-inflammatory and anti-inflammatory responses.²⁶ Likewise, certain extracellular histones are involved in activating the immune system.^{31,32} Lastly, C9, a component of the MAC, was upregulated. However, there was no significant complement deposit on muscle fibers on MAC staining. It is possible that the amount of deposited complement escaped detection by the used immunofluorescent method.

In addition to the immune-related proteins, which were the focus of our study, we also identified significant changes in several proteins implicated in muscle function. As expected, downregulated muscle proteins consisted mostly of structural contractile and sarcomeric proteins. In contrast, a wide array of proteins involved in DNA transcription, RNA translation, protein synthesis and homeostasis, cell adhesion, actin dynamics, and cell metabolism were upregulated. These proteins overlap with

those detected in other inherited myopathies with cytoplasmic aggregates such as myofibrillar myopathies, or acquired myopathies such as inclusion body myositis, and rare reports from congenital nemaline myopathy mouse models.^{33–38} Therefore, these proteins probably reflect converging pathomechanisms indicating muscle fiber injury, unlike immune-related proteins which are rarely encountered in inherited myopathies.^{34–38} Regarding the most common category of nuclear proteins, this is in keeping with the findings on muscle biopsy, where fibers with rods often display internalized nuclei with prominent nucleoli, reflecting high (compensatory) protein synthesis. However, there may be some contribution from sampling bias, as it may be easier to avoid nuclei in normal fibers given their clear subsarcolemmal location. Conversely, in fibers with rods, nuclei may sometimes be difficult to dissect from surrounding sarcoplasmic material.

Our study was limited by the small sample size and the scarce available literature on SLONM pathogenesis.

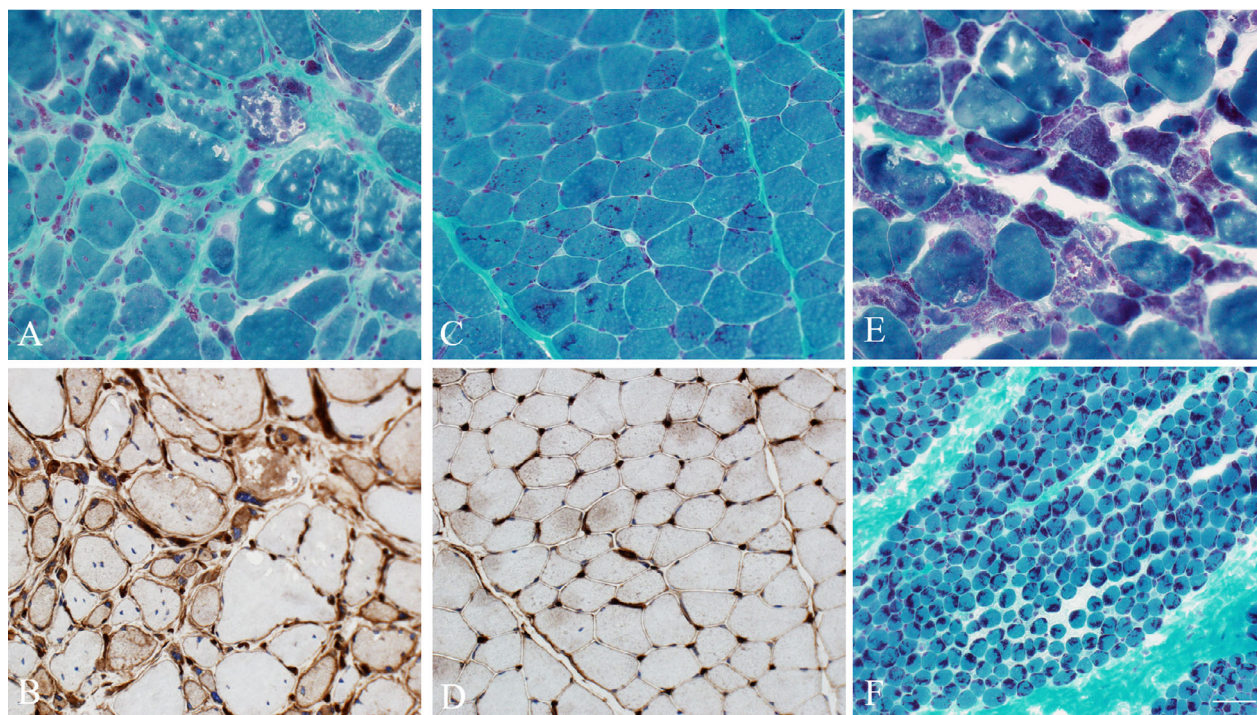


Figure 1. Muscle biopsy findings. Trichrome-stained frozen sections (A, C, E, and F) and MHC1-reacted sections (B and D) from patients with SLOM (A, B, and E) and patients with congenital nemaline myopathy (C, D, and F). In SLOM patients, increased MHC1 reactivity was present in fibers containing nemaline rods as well as adjacent nonatrophic fibers (B), whereas fibers containing nemaline rods from patients with congenital nemaline myopathy did not display increased MHC1 reactivity (D). In SLOM, nemaline rods tend to accumulate in atrophic fibers (A and E) with marked rarefaction of the myofibrils. Whereas in congenital nemaline myopathies, nemaline rods occur in nonatrophic fibers and occur subsarcolemmally (F) or scattered throughout the sarcoplasm (C). Scale bar: 50 μ m. MHC1, major histocompatibility complex 1; SLOM, sporadic late-onset nemaline myopathy.

Limitations also included those inherent to the proteomics platform and the depth of coverage of the utilized equipment and methods. Furthermore, the high dynamic range in muscle (over-abundance of muscle structural proteins in the samples) makes it more difficult to see less abundant proteins. The omics platforms provide immense amount of data that may be difficult to interpret and to determine their clinical relevance. Future studies should include integration with other omics' platform to better understand SLOM pathogenesis. It would also be helpful to compare the findings in SLOM to other myopathies, namely congenital nemaline myopathy and idiopathic inflammatory myopathies. Moreover, comparing the IGV of the circulating clonal plasma cells, which would require PCR of clonal bone marrow plasma cells, to the detected IGVs in tissue would be of interest.

Acknowledgments

The authors acknowledge their colleagues in Neurology and Hematology who contributed to the care of the published patients.

Conflict of Interest

Elie Naddaf, Surendra Dasari, Duygu Selcen, M. Cristine Charlesworth, Kenneth L Johnson, Michelle L. Mauermann, and Taxiarchis Kourelis report no conflict of interest.

References

1. Naddaf E, Milone M, Kansagra A, Buadi F, Kourelis T. Sporadic late-onset nemaline myopathy: clinical spectrum, survival, and treatment outcomes. *Neurology*. 2019;93(3): e298-e305. doi:10.1212/wnl.0000000000000777
2. Schnitzler LJ, Schreckenbach T, Nadaj-Pakleza A, et al. Sporadic late-onset nemaline myopathy: clinicopathological characteristics and review of 76 cases. *Orphanet J Rare Dis*. 2017;12(1):86. doi:10.1186/s13023-017-0640-2
3. Engel AG. Late-onset rod myopathy (a new syndrome?): light and electron microscopic observations in two cases. *Mayo Clin Proc*. 1966;41(11):713-741.
4. Engel WK, Oberc MA. Abundant nuclear rods in adult-onset rod disease. *J Neuropathol Exp Neurol*. 1975;34(2):119-132. doi:10.1097/00005072-197503000-00001

5. Chahin N, Selcen D, Engel AG. Sporadic late onset nemaline myopathy. *Neurology*. 2005;65(8):1158-1164. doi:10.1212/01.wnl.0000180362.90078.dc
6. Kyle RA, Therneau TM, Rajkumar SV, et al. Prevalence of monoclonal gammopathy of undetermined significance. *N Engl J Med*. 2006;354(13):1362-1369. doi:10.1056/NEJMoa054494
7. Monforte M, Primiano G, Silvestri G, et al. Sporadic late-onset nemaline myopathy: clinical, pathology and imaging findings in a single center cohort. *J Neurol*. 2018;265(3):542-551. doi:10.1007/s00415-018-8741-y
8. Voermans NC, Minnema M, Lammens M, et al. Sporadic late-onset nemaline myopathy effectively treated by melphalan and stem cell transplant. *Neurology*. 2008;71(7):532-534. doi:10.1212/01.wnl.0000310814.54623.6f
9. Voermans NC, Benveniste O, Minnema MC, et al. Sporadic late-onset nemaline myopathy with MGUS: long-term follow-up after melphalan and SCT. *Neurology*. 2014;83(23):2133-2139. doi:10.1212/wnl.0000000000001047
10. Tanboon J, Uruha A, Arahata Y, et al. Inflammatory features in sporadic late-onset nemaline myopathy are independent from monoclonal gammopathy. *Brain Pathol*. 2021;31(3):e12962. doi:10.1111/bpa.12962
11. Ayers-Ringler JR, Oliveros A, Qiu Y, et al. Label-free proteomic analysis of protein changes in the striatum during chronic ethanol use and early withdrawal. *Front Behav Neurosci*. 2016;10:46. doi:10.3389/fnbeh.2016.00046
12. Tyanova S, Temu T, Cox J. The MaxQuant computational platform for mass spectrometry-based shotgun proteomics. *Nat Protoc*. 2016;11(12):2301-2319. doi:10.1038/nprot.2016.136
13. Subramanian A, Tamayo P, Mootha VK, et al. Gene set enrichment analysis: a knowledge-based approach for interpreting genome-wide expression profiles. *Proc Natl Acad Sci USA*. 2005;102(43):15545-15550. doi:10.1073/pnas.0506580102
14. Kourelis TV, Dasari S, Theis JD, et al. Clarifying immunoglobulin gene usage in systemic and localized immunoglobulin light-chain amyloidosis by mass spectrometry. *Blood*. 2017;129(3):299-306. doi:10.1182/blood-2016-10-743997
15. Li M, Gray W, Zhang H, et al. Comparative shotgun proteomics using spectral count data and quasi-likelihood modeling. *J Proteome Res*. 2010;9(8):4295-4305. doi:10.1021/pr100527g
16. Wiczorek M, Abualrous ET, Sticht J, et al. Major histocompatibility complex (MHC) class I and MHC class II proteins: conformational plasticity in antigen presentation. *Front Immunol*. 2017;8:292. doi:10.3389/fimmu.2017.00292
17. Díaz-Muñoz MD, Turner M. Uncovering the role of RNA-binding proteins in gene expression in the immune system. *Front Immunol*. 2018;9:1094-1094. doi:10.3389/fimmu.2018.01094
18. Le Bras S, Foucault I, Foussat A, Brignone C, Acuto O, Deckert M. Recruitment of the actin-binding protein HIP-55 to the immunological synapse regulates T cell receptor signaling and endocytosis. *J Biol Chem*. 2004;279(15):15550-15560. doi:10.1074/jbc.M312659200
19. Castaneda-Avila MA, Ulbricht CM, Epstein MM. Risk factors for monoclonal gammopathy of undetermined significance: a systematic review. *Ann Hematol*. 2021;100(4):855-863. doi:10.1007/s00277-021-04400-7
20. Dasari S, Theis JD, Vrana JA, et al. Proteomic detection of immunoglobulin light chain variable region peptides from amyloidosis patient biopsies. *J Proteome Res*. 2015;14(4):1957-1967. doi:10.1021/acs.jproteome.5b00015
21. Vrana JA, Gamez JD, Madden BJ, Theis JD, Bergen HR III, Dogan A. Classification of amyloidosis by laser microdissection and mass spectrometry-based proteomic analysis in clinical biopsy specimens. *Blood*. 2009;114(24):4957-4959. doi:10.1182/blood-2009-07-230722
22. Bodi K, Prokaeva T, Spencer B, Eberhard M, Connors LH, Seldin DC. AL-base: a visual platform analysis tool for the study of amyloidogenic immunoglobulin light chain sequences. *Amyloid*. 2009;16(1):1-8. doi:10.1080/13506120802676781
23. Naddaf E, Kourelis T. Comments on: chemotherapy-based approach is the preferred treatment for sporadic late-onset nemaline myopathy with a monoclonal protein. *Int J Cancer*. 2021;149(3):741-742. doi:10.1002/ijc.33572
24. Mihara K, Wong NCW. 369. Activation of killer T cells by TGF-beta antagonist, alpha 2-HS glycoprotein. *Mol Ther*. 2002;5(5):S121-S122. doi:10.1016/S1525-0016(16)43199-0
25. West KO, Scott HM, Torres-Odio S, West AP, Patrick KL, Watson RO. The splicing factor hnRNP M is a critical regulator of innate immune gene expression in macrophages. *Cell Rep*. 2019;29(6):1594-1609.e5. doi:10.1016/j.celrep.2019.09.078
26. Zininga T, Ramatsui L, Shonhai A. Heat shock proteins as immunomodulators. *Molecules*. 2018;23(11):2846. doi:10.3390/molecules23112846
27. Honkala AT, Tailor D, Malhotra SV. Guanylate-binding protein 1: an emerging target in inflammation and cancer. *Front Immunol*. 2019;10:3139. doi:10.3389/fimmu.2019.03139
28. Rayavarapu S, Coley W, Kinder TB, Nagaraju K. Idiopathic inflammatory myopathies: pathogenic mechanisms of muscle weakness. *Skelet Muscle*. 2013;3(1):13. doi:10.1186/2044-5040-3-13
29. Allenbach Y, Chhara W, Rosenzweig M, et al. Th1 response and systemic treg deficiency in inclusion body myositis. *PLoS One*. 2014;9(3):e88788. doi:10.1371/journal.pone.0088788
30. Preuße C, Goebel HH, Held J, et al. Immune-mediated necrotizing myopathy is characterized by a specific Th1-M1 polarized immune profile. *Am J Pathol*. 2012;181(6):2161-2171. doi:10.1016/j.ajpath.2012.08.033

31. Silk E, Zhao H, Weng H, Ma D. The role of extracellular histone in organ injury. *Cell Death Dis.* 2017;8(5):e2812-e2812. 10.1038/cddis.2017.52
32. Hoeksema M, van Eijk M, Haagsman HP, Hartshorn KL. Histones as mediators of host defense, inflammation and thrombosis. *Future Microbiol.* 2016;11(3):441-453. 10.2217/fmb.15.151
33. Güttsches AK, Brady S, Krause K, et al. Proteomics of rimmed vacuoles define new risk allele in inclusion body myositis. *Ann Neurol.* 2017;81(2):227-239. 10.1002/ana.24847
34. Maerkens A, Kley RA, Olivé M, et al. Differential proteomic analysis of abnormal intramyoplasmic aggregates in desminopathy. *J Proteome.* 2013;90:14-27. 10.1016/j.jprot.2013.04.026
35. Maerkens A, Olivé M, Schreiner A, et al. New insights into the protein aggregation pathology in myotilinopathy by combined proteomic and immunolocalization analyses. *Acta Neuropathol Commun.* 2016;4:8-8. 10.1186/s40478-016-0280-0
36. Kley RA, Leber Y, Schrank B, et al. FLNC-associated myofibrillar myopathy: new clinical, functional, and proteomic data. *Neurol Genet.* 2021;7(3):e590. 10.1212/nxg.0000000000000590
37. Yamamoto DL, Vitiello C, Zhang J, et al. The nebulin SH3 domain is dispensable for normal skeletal muscle structure but is required for effective active load bearing in mouse. *J Cell Sci.* 2013;126(Pt 23):5477-5489. 10.1242/jcs.137026
38. Gineste C, De Winter JM, Kohl C, et al. In vivo and in vitro investigations of heterozygous nebulin knock-out mice disclose a mild skeletal muscle phenotype. *Neuromuscul Disord.* 2013;23(4):357-369. 10.1016/j.nmd.2012.12.011

Supporting Information

Additional supporting information may be found online in the Supporting Information section at the end of the article.

Table S1. Complete list of differentially expressed proteins in sporadic late-onset nemaline myopathy.

Table S2. Immunoglobulin heavy and light chain proteins.

Data S1. R script file.